

Cosmic-gamma-ray emission at low-luminosity from CCO 1E 1207.4-5209 and its Host SNR G296.5+10.0

Luana N. Padilha,^{a,1} Rita C. dos Anjos,^{a,b,c,d} Jaziel G. Coelho,^{d,e} Luiz A. S. Pereira^f

^aPrograma de pós-graduação em Física & Departamento de Física, Universidade Estadual de Londrina (UEL), 86057-970 Londrina, PR, Brazil

^bDepartamento de Engenharias e Exatas, Universidade Federal do Paraná (UFPR), Pioneiro, 2153, 85950-000 Palotina, PR, Brazil

^cApplied Physics Graduation Program, Federal University of Latin-American Integration, 85867-670, Foz do Iguaçu, PR, Brazil

^dNúcleo de Astrofísica e Cosmologia (Cosmo-Ufes) & Departamento de Física, Universidade Federal do Espírito Santo, 29075-910, Vitória, ES, Brazil

^eDivisão de Astrofísica, Instituto Nacional de Pesquisas Espaciais, Avenida dos Astronautas 1758, 12227-010, São José dos Campos, SP, Brazil

^fUnidade Acadêmica de Física, Universidade Federal de Campina Grande, 58429-900, Campina Grande, PB, Brazil

E-mail: luana.natalie.padilha@uel.br, ritacassia@ufpr.br, jaziel.coelho@ufes.br, luizstuani@uaf.ufcg.edu.br

Abstract. The origin and acceleration mechanisms of energetic particles in the universe remain enigmatic in contemporary astrophysics. Recent efforts have focused on identifying Galactic sources capable of accelerating particles to 1 PeV, known as PeVatrons, and also identifying sources contributing to the spectrum at lower energies. The different morphology of galactic supernova remnants is directly related to the type of stellar explosion and the existence of a possible Compact Central Object (CCO), which possess intense radiative-gravitational fields on their surfaces. These CCOs, due to their strong fields and interactions with surrounding magnetic clouds, are potential candidates for gamma ray production. Through observations of the compact X-ray source 1E 1207.4-5209, located near the remnant G296.5+10.0, and using the enhanced GALPROP code, we analyze the emission of gamma-ray and cosmic-ray production through propagation. Additionally, we calculate the contribution of the G296.5+10.0 source to the overall observed Galactic cosmic-ray flux, taking into account cosmic-ray propagation within the Galaxy, which includes energy losses and particle interactions. Our findings suggest that this setup offers a fertile environment for producing a wide range of cosmic-ray energies at low energy within the Galaxy.

¹Corresponding author.

Contents

1	Introduction	1
2	CCO 1E 1207.4-5209 and its host SNR G296.5 + 10.0	2
3	Description of simulation models	3
4	Discussions	5
5	Summary	6

1 Introduction

Extensive research has revealed that many astrophysical objects within our galaxy are neutron stars (NS). Intriguingly, these discoveries often align with the locations of Supernova Remnants (SNRs) [1]. These sources, known as Compact Central Objects (CCOs), are identifiable by their intense thermal X-ray emissions and a notable absence of radio and gamma-ray emissions [2]. In particular, CCOs exhibit characteristics [see 3, 4] that make them ideal candidates for particle acceleration at extremely high energies. This potential is amplified by the fact that CCOs and their associated supernova remnants provide an excellent opportunity to integrate kinematic data from both the neutron star and the supernova shock wave [1].

Supernova remnants and the potential presence of compact central object CCOs are inherently linked to the type of explosion of the progenitor star. Consequently, they exhibit distinct morphologies, often influenced by the materials in their vicinity and the compression of diverse magnetic fields [5]. CCOs are astronomical entities located at the geometric centers of supernova remnants, characterized by thermal X-ray emissions in the hundreds of electronvolts (eV) range and luminosities ranging from 10^{33} to 10^{34} (erg/s^{-1}) [see, e.g., 6, 7]. An intriguing characteristic of these objects is their minimal emissions in alternative energy bands [2, 7, 8]. Due to their elusive nature, only ten CCOs have been officially cataloged, with many more potentially existing but not yet discovered [see, e.g., 1]. Measurements of their rotational periods and decay rates indicate that these objects possess antimagnetic properties, with weak magnetic fields spanning the range of 10^{10} to 10^{11} G. These weak magnetic fields likely result from magnetic dipole braking, suggesting that CCOs are relatively young entities [see, e.g., 9].

Multimessenger astronomy approaches to the origin search of cosmic rays (CRs) are based on the inclusion of all available information from charged CRs and neutral secondaries generated near sources by interactions. In particular, neutron and gamma rays flux through the interaction of CRs with fields. Furthermore, accelerated electrons and positrons can produce radiation through the synchrotron emission, bremsstrahlung and Inverse Compton [10, 11]. The relationship between the propagation of cosmic rays and the integral flux of secondary gamma-rays from a source determined cosmic ray luminosities in models both inside and outside of our Galaxy [12–16].

This paper calculates the contribution of the secondary gamma rays from charge particles by the CCO 1E 1207.4-5209 and its host SNR G296.5 + 10.0 association [17] using the v57 GALPROP release [18] with 3D maps of the Galactic magnetic field, diffuse interstellar

medium (ISM) distributions, the interstellar radiation field (ISRF), and the gas distribution throughout the Galaxy. Our simulation model centers on CCO 1E 1207.4-5209 parameters, distinguished by their measured magnetic field. The description of the source is given precedence according to predetermined criteria, including location, age, period variation, and luminosity.

This study was motivated by the coexistence of CCO 1E 1207.4-5209 within the vicinity of its host SNR G296.5+10.0 [17]. SNR G296.5+10.0 has been widely investigated as a high energy gamma-ray emitter, with a focus on the lepto-hadronic spectral energy distribution of the remnant for synchrotron, inverse Compton, Bremsstrahlung, and proton-proton processes [19–21]. In this context, this work aims to quantify a potential gamma-ray emission from the SNR G296.5+10.0 and CCO 1E 1207.4-5209 to the region, which cannot be ignored due to glitch processes associated with the spin-down rate [22] and changes in the pulsar’s spin period [23].

This manuscript is organized as follows. The next section presents in detail the association CCO 1E 1207.4-5209 and its host SNR G296.5 + 10.0. The third section presents the description of simulation models. Beyond that, in this section we describe our multi-messenger analysis. The final section provides the main conclusions and discussions of this investigation.

2 CCO 1E 1207.4-5209 and its host SNR G296.5 + 10.0

The neutron star 1E 1207.4-5209 is a radio-quiet, fast-rotating object of the CCO class [24], which was detected near the core of SNR G296.5+10.0 by the Einstein satellite [25]. Situated at the geometric center of the supernova remnant G296.5+10.0 (also named PKS 1209-51), the CCO 1E 1207.4-5209 was the focus of a comprehensive XMM-Newton spacecraft observation in August 2002 [26]. Using the EPIC 12,13 instrument, the observations lasted approximately 36 hours and significantly advanced the study of its emission [27]. This CCO possesses a rotational period of 0.42413076 seconds, and its period derivative is constrained by an upper limit of $2.224 \times 10^{-17} \text{ s; s}^{-1}$ (according to the ATNF catalog¹). Situated in the Centaurus constellation, it is positioned at a distance of 2 kiloparsecs [28]. As reported by [27], the light curve of this object spans an energy range from 0.2 to 4 keV.

It is the second isolated neutron star (INS) candidate discovered inside a supernova remnant (SNR) thermally emitting [17]. The supernova remnant G296.5+10.0 exhibits intense X-ray and radio emissions concentrated in the southern, eastern, and southwestern regions [29]. It possesses a bilateral morphology, with symmetry axes parallel to the Galactic plane and two bright arms on the sides. Some experts suggest that the remnant features tangentially positioned filaments composed of compressed cold gas clouds [see 30], along with a shell consisting of H_I [31].

The pulsar 1E 1207.4-5209 is widely recognized as the first to exhibit strong absorption lines. It was suggested that a young age and a low level of magnetospheric activity are favorable conditions for detecting atomic spectral features of elements with $Z > 1$ [26]. In older objects, these elements would be overlaid by a thin layer of accumulated hydrogen or masked by non-thermal processes in young and energetic pulsars. Following that, the possible composition of the atmosphere was tightly restricted by subsequent research [32], indicating that the absorption characteristics are naturally linked to oxygen or neon with helium-like properties in a magnetic field of around $\sim 10^{12}$ G. Consequently, pulsar’s magnetosphere is

¹<https://www.atnf.csiro.au/research/pulsar/psrcat/>

an environment rich in positrons and electrons and is subjected to acceleration through the pulsar’s spin-down mechanism.

This source stands out as a unique computational neutron star in which the magnetic field is directly measured, rather than being inferred, as in other objects of its class. The XMM-Newton telescope detected X-ray absorption lines in its spectrum, which can be interpreted as cyclotron resonance of electrons near the central object’s surface. The cyclotron lines (0.7 keV) correspond to a magnetic field of approximately 8×10^{10} G or 1.6×10^{14} G [see 9, 27, 33, 34]. Another intriguing characteristic of this CCO is its age, as it is believed to have formed simultaneously with the associated supernova remnant, given its origin linked to the death of the progenitor star. However, the remarkable age of 1E 1207.4-5209 exceeds by three orders of magnitude the age of the supernova G296.5+10.0. This suggests the presence of a significant braking index, especially if the current rotation period of the star is approximated to its characteristic period [see, e.g., 33]. These features make this CCO notable among other known pulsars.

3 Description of simulation models

In its most recent version 57, the GALPROP program was utilized to create a realistic model. GALPROP solves the transport equation, Eq. 3.1, for a given source distribution while accounting for all spatial and energetic processes that the particles encounter during propagation [18].

$$\frac{\partial N}{\partial t} = Q(\mathbf{x}, p) + \vec{\nabla} \cdot (D_{xx} \vec{\nabla} N - \vec{v} N) + \frac{\partial}{\partial p} p^2 D_{pp} \frac{\partial}{\partial p} \frac{1}{p^2} N - \frac{\partial}{\partial p} (\dot{p} N - \frac{p}{3} (\vec{\nabla} \cdot \vec{v}) N) - \sum_{i=1}^2 \frac{N}{\tau_i}, \quad (3.1)$$

where Q is a source term for the injection of cosmic rays, including secondary creation of cosmic rays, and $N(x, p)$ is the density of cosmic rays per unit of total particle momentum. The spatial diffusion coefficient in our model is D_{xx} , the convection velocity is \vec{v} , and the time scales for radioactive decay (τ_1) and fragmentation (τ_2). A power law with an index δ determines the diffusion coefficient, which is a scalar function homogeneous and isotropic throughout the Galaxy. It is expressed as $D_{xx} = \beta D_{0,xx} (\rho/\rho_0)^\delta$, where $\rho_0 = 3$ GV, $D_{0,xx}$ is a diffusion constant, and β is the velocity expressed in units of light speed. The convection velocity $\vec{v}(z)$ is assumed to increase linearly with the distance z between the plane and the halo. In a single zone $|z| > 1$ kpc, cosmic-ray propagation is diffusive-convective [35]. At low energies, up to ~ 1 GeV [36], both galactic wind and energy losses play a significant role. A momentum diffusion coefficient D_{pp} determines the re-acceleration. It is related to the spatial coefficient D_{xx} via $D_{pp} \propto p^2 v_a^2 / D_{xx}$, where the Alfvén speed is denoted by v_a , the momentum loss rate is $\dot{p} \equiv dp/dt$, and the Kolmogorov spectrum of turbulence is taken into account.

The transport equation is solved by the software using the Crank-Nicholson model of second order. Utilizing source abundance relations for isotope generation and the boron-carbon ratio in terms of the stiffness and dispersion characteristics, the diffusion coefficient is computed [see 16, for details]. The Galactic gas distribution was modeled using a high column density H model [37]. Energy losses from synchrotron and Compton scattering processes are taken into account by the GALPROP code, which calculates the losses using an observer centered on the solar system. Furthermore, the interstellar radiation field is modeled using an R12 model [see 38]. For the Galactic magnetic field, a basic exponential model is taken

into account [39]. The magnetic field has cylindrical symmetry and was chosen to describe the synchrotron emission: $B(r, z) = B_0 e^{(R_\odot - r)/R_B} e^{-|z|/z_B}$ [40], where $R_\odot = 8.5$ kpc is the Solar Radius, $B_0 = 5\mu G$, $R_B = 6$ kpc and $z_B = 2$ kpc are the radial and vertical scale lengths [41]. This model only accounts the random magnetic field distribution, which is related to the diffusive features of cosmic rays [42, 43]. The current model cannot account for significant magnetic fields near the galactic core [44]. An overview of the simulation parameters is provided in Table 1. The source function $Q(\mathbf{x}, p)$ is written as $n(\mathbf{x})q(p)$, where

Table 1: Simulation parameters

Parameters	Values	Units
Grid	$\begin{cases} x & -18.0 : +18.0 \\ y & -18.0 : +18.0 \\ z & -4.0 : +4.0 \end{cases}$	kpc
E_{min}	1	MeV
E_{max}	1.0×10^{11}	MeV
$D_{0,xx}$	2.5×10^{28}	$\text{cm}^2 \text{s}^{-1}$
v_a	28.0	km s^{-1}

$n(\mathbf{x})$ is the amount of energy injected by cosmic rays and electrons/positrons and $q(p)$ is their spatial distribution. We use a differential injection spectrum that is based on a power law for momentum $dq(p)/dp \propto p^{-\alpha}$, characterized by indices of 2.2 - 2.6 [45, 46]. The Models inject particles following a δ -function centered at the source.

The spin-down model was the initial emission model considered for CCO 1E 1207.4-520. In this scenario, dipole radiation is responsible for the pulsar’s power loss and electron acceleration. We consider the contribution of a continuous source of energetic particles (electrons and positrons) to the spatial distribution at the position of the CCO 1E 1207.4-5209 vicinity. With an injection power that follows a power law with a smooth break and accelerated acceleration, the model implies that the spectrum is normalized by [16, 18, 47, 48]

$$L(t) = \eta L_0 \left(1 + \frac{t}{\tau_0} \right)^{-2}, \quad (3.2)$$

where $L_0 = 1.0 \times 10^{33} \text{ erg s}^{-1}$ [27, 28] is the initial rotational power of the source, $\eta = 1$ is the efficiency, and $\tau_0 = 3.63 \times 10^5 \text{ yr}$ is the time scale of the pulsar ². The rate of cosmic-ray production correlates with the spin down of pulsars [see 16, 48].

The second model utilizes quiescent emission or magnetic energy injection to generate a cosmic-ray luminosity and afterwards derives a gamma-ray luminosity based on the upper limits set by the H.E.S.S. Collaboration [21]. Fermi-accelerated protons lose their energy by hadronic interaction (p-p), producing neutral pions that decay into photons and form the primary source of gamma-ray observations. Depending on the energy of the gamma rays, they can be observed with space- and ground-based instruments [49]. Very high gamma-ray emission (VHE) can result from interactions between protons or electrons, matter, and radiation. Extragalactic models suggest that the relationship between the total flux of GeV-TeV gamma rays emitted by a source and the propagation of cosmic rays can establish an

²In the magnetic dipole approximation, we can utilize an equation relating rotation rate, characteristic age, and a specific time scale to calculate the initial rotational energy. This is valuable for estimating the initial energy of neutron stars, taking into account their standard parameters [16, 48]

upper limit on the overall luminosity of cosmic rays [12, 13]. Some sources have only an upper limit on the integral of the gamma-ray flux provided. For these objects, the upper limit constrains the total of the primary and secondary photon fluxes. We assume that the measured upper limit flux of GeV-TeV gamma rays is regarded as the upper limit on secondary gamma rays created by cosmic rays traveling from a distant source to Earth. In that case, we can determine the cosmic-ray luminosity.

This paper presents an approach that establishes a correlation between the cosmic-ray luminosity and a measured upper limit to the integral flux of GeV-TeV gamma rays from SNR G296.5+10.0. An isotropic cosmic-ray emission is assumed. The luminosity of the cosmic-ray flux of SNR G296.5+10.0 is directly proportional to the secondary gamma-ray flux it generates. The gamma-ray production per unit volume is conservative and can be expressed as the following function of cosmic-ray luminosity:

$$I_\gamma(E_\gamma) \sim n_{\text{gas}} \frac{W_{\text{CR}}}{4\pi d^2 \langle E_0 \rangle} K_\gamma P_\gamma(E_\gamma), \quad (3.3)$$

where W_{CR} is the total energy of the nuclei, n_{gas} is the gas number density, and $\langle E_0 \rangle$ is the average energy, E_γ is the gamma-ray energy, and K_γ and $P_\gamma(E_\gamma)$ are the gamma-ray number from cosmic-ray propagation and the gamma-ray energy distribution recorded on Earth, respectively [15, 16, 50, 51].

The upper limit of $(1.19 \pm 0.11) \times 10^{-9} \text{ cm}^{-2} \text{ s}^{-1}$ for the integral flux in the 1 GeV < E < 1 TeV range was obtained by H.E.S.S at the confidence level (CL) 99.5% [21]. The secondary gamma-ray flux generated by SNR G296.5 + 10.0 is proportional to its cosmic-ray flux or luminosity, according to the previously established model. The results derived for the gamma-ray emission and spectral energy distribution from these models are discussed in the following section. The simulations are based on the parameters of the association CCO 1E 1207.4-5209 + SNR G296.5+10.0.

4 Discussions

This section contains the results of the transport models we developed. We begin by analyzing the spectra distributions of four elements in cosmic rays using distinct model emission. The 2D gas distribution of the interstellar gas was used to simulate the models [38, 52]. Figure 1 shows the spectral energy distribution of the gamma-ray emissions resulting from the proton in Supernova Remnant (SNR) G296.5 + 10.0 and electron/positron from CCO at the spectral indexes of 2.2 (a), 2.4 (b) and 2.6 (c). A range of values between 2.0 and 2.6 was selected according to the spectrum of individual sources and observations as described in [15, 45]. The key observation is that the CCO exerts a considerable influence on gamma rays in its vicinity at high energies ($E > 10^6$ MeV) through the inverse Compton process, as depicted in Figure 1-(c). It may be inferred that the rotating properties of the object lead to an injection power of electrons.

The plot 1 illustrates the poor gamma-ray data/model of CCO 1E 1207.4-5209 and its corresponding Supernova Remnant (SNR) G296.5 + 10.0. This is based on the model proposed by [21] and the gamma-ray measurements conducted by [53]. The lines indicate a larger fraction of gamma radiation emission in the energy range of $10^2 - 10^5$ MeV, where the simulation data meet the CCO gamma emission data [53], for all spectral indexes in Fig. 1-(a,b,c). In the spin-down scenario, gamma-ray emission is mostly produced by Inverse Compton.

Figures 2 and 3 show the energy spectra for proton and other elements, respectively. The Fig. 2 describes how the source contributes to the overall proton cosmic ray flux, considering three different spectral indices: 2.2 (see Fig. 2 - (a)), 2.4 (see Fig. 2 - (b)), and 2.6 (see Fig. 2 - (c)). The spectra demonstrated in Fig. 3 follow a pattern similar to that of Fig. 2. However, as expected, the impact of the source on the spectra of heavier elements is significantly diminished as a result of the reduced flux of these particles. The presence of a Central Compact Object (CCO) associated with a supernova event could lead to the emission of charged and multi-messenger particles at low energy. However, we have no evidence of nucleus acceleration by CCO [25]. Figure 4 illustrates the impact of source on electron and positron emissions compared to measurements from various experiments, and the spin-down model once more gives a contribution at $E > 10^6$ eV.

The B/C ratio against the kinetic energy per nucleon for our models compared to the CR data is shown in Fig. 5. Since there is only one region source, the purpose of this illustration was not to elucidate the data. Instead, its objective was to establish a comparison between the contributions of the emission models to gamma-ray emission. Moreover, it becomes apparent that the spin-down contribution is effective in contributing with data. The main result indicates that although the association between CCO 1E 1207.4-5209 and its host SNR G296.5+10.0 contributes to the low energy gamma-ray spectrum, it is inefficient in accelerating particles to high energies. Finally, we investigate the impact of the gas distribution on the total predicted gamma-ray intensity for the spin-down model in Figure 6. The impact of alternate gas maps on the spectrum is discussed in detail in [46]. The figures depict the intensity calculated at both 1 GeV and 1 TeV for electron emissions through inverse Compton and bremsstrahlung processes, utilizing the 3D gas model. The three-dimensional spatial density model for neutral and molecular hydrogen was developed based on gas line-survey data [37]. There is an increase in intensity at 1 TeV for both inverse Compton and bremsstrahlung processes.

5 Summary

In this study, we generated gamma-ray spectra from particles through simulations involving the association of the only pulsar with an inferred magnetic field, CCO 1E 1207.4-5209, and the supernova remnant G296.5 + 10.0. We considered two different emission scenarios at the source. Our findings are a direct result of energy particle propagation processes up to 10^{14} eV, emphasizing the need to construct and assess propagation models to understand the physics of Galactic cosmic rays and the emission zone of sources inside our Galaxy. The spin-down model contributed to our findings and showed that this CCO 1E 1207.4-5209, with its measured magnetic field, can contribute to the spectrum of gamma rays only at low energy.

Another outcome demonstrating the inefficiency of association in acceleration is that, even when using the upper limit of the energy integral range in GeV-TeV, the resulting model favored a low-luminosity scenario. The association does not significantly impact the particle spectrum. However, the limited source emission data currently available restrict us from drawing more comprehensive conclusions. In the future, Cherenkov Telescope Array Observatory (CTAO) measurements [see 54] will offer enhanced insights and opportunities for modeling emissions from this CCO and other low gamma emission sources.

Acknowledgments

We thank the anonymous referee for providing valuable suggestions, which helped improve this work. This study was financed in part by the Coordenação de Aperfeiçoamento de Pessoal de Nível Superior – Brasil (CAPES) – Finance Code 001. J.G.C. is grateful for the support of FAPES (1020/2022, 1081/2022, 976/2022, 332/2023) and CNPq (311758/2021-5). The research of R.C.A. is supported by Conselho Nacional de Desenvolvimento Científico e Tecnológico (CNPq), grant number 310448/2021-2. R.C.A. and L.N.P are grateful for the support of L’Oreal Brazil, with partnership of ABC and UNESCO in Brazil. The authors acknowledge the National Laboratory for Scientific Computing (LNCC/MCTI, Brazil) for providing HPC resources of the SDumont supercomputer, which have contributed to the research results reported in this paper. URL: <http://sdumont.lncc.br>. J.G.C and R.C.A acknowledge the financial support of FAPESP Project No. 2021/01089-1. The authors acknowledge the financial support of NAPI *Fenômenos Extremos do Universo* of Fundação de Apoio a Ciência, Tecnologia e Inovação do Paraná.

References

- [1] M.G.F. Mayer and W. Becker, *A kinematic study of central compact objects and their host supernova remnants*, *A&A* **651** (2021) A40 [2106.00700].
- [2] A.K. Harding, *The neutron star zoo*, *Frontiers of Physics* **8** (2013) 679 [1302.0869].
- [3] A.M. Hillas, *Where do 10^{19} eV cosmic rays come from?*, *Nuclear Physics B Proceedings Supplements* **136** (2004) 139.
- [4] K.V. Ptitsyna and S.V. Troitsky, *Physical conditions in potential accelerators of ultra-high-energy cosmic rays: updated Hillas plot and radiation-loss constraints*, *Physics Uspekhi* **53** (2010) 691 [0808.0367].
- [5] L.A. Lopez and R.A. Fesen, *The Morphologies and Kinematics of Supernova Remnants*, *Space Science Reviews* **214** (2018) 44 [1804.00024].
- [6] J.P. Halpern and E.V. Gotthelf, *Spin-Down Measurement of PSR J1852+0040 in Kesteven 79: Central Compact Objects as Anti-Magnetars*, *ApJ* **709** (2010) 436 [0911.0093].
- [7] G.G. Pavlov, D. Sanwal and M.A. Teter, *Central Compact Objects in Supernova Remnants*, in *Young Neutron Stars and Their Environments*, F. Camilo and B.M. Gaensler, eds., vol. 218, p. 239, Jan., 2004, DOI [astro-ph/0311526].
- [8] A. De Luca, *Central compact objects in supernova remnants*, in *Journal of Physics Conference Series*, vol. 932 of *Journal of Physics Conference Series*, p. 012006, Dec., 2017, DOI [1711.07210].
- [9] J.P. Halpern and E.V. Gotthelf, *Spin-Down Measurement of PSR J1852+0040 in Kesteven 79: Central Compact Objects as Anti-Magnetars*, *ApJ* **709** (2010) 436 [0911.0093].
- [10] J. Becker Tjus, *Search for Galactic cosmic ray sources: The multimessenger approach*, in *European Physical Journal Web of Conferences*, vol. 105 of *European Physical Journal Web of Conferences*, p. 00003, Dec., 2015, DOI.
- [11] J. Becker Tjus and L. Merten, *Closing in on the origin of Galactic cosmic rays using multimessenger information*, *Physics Reports* **872** (2020) 1 [2002.00964].
- [12] A.D. Supanitsky and V. de Souza, *An upper limit on the cosmic-ray luminosity of individual sources from gamma-ray observations*, *JCAP* **2013** (2013) 023 [1311.4820].
- [13] R.C. Anjos, V. de Souza and A.D. Supanitsky, *Upper limits on the total cosmic-ray luminosity of individual sources*, *JCAP* **2014** (2014) 049 [1405.3937].

- [14] R. Sasse and R.C. dos Anjos, *Upper limits on the cosmic-ray luminosity of supernovae in nearby galaxies*, in *37th International Cosmic Ray Conference*, p. 461, Mar., 2022, DOI.
- [15] R.C. dos Anjos, J.G. Coelho, J.P. Pereira and F. Catalani, *High-energy gamma-ray emission from SNR G57.2+0.8 hosting SGR J1935+2154*, *JCAP* **2021** (2021) 023 [2106.03008].
- [16] J.G. Coelho, L.N. Padilha, R.C. dos Anjos, C.V. Ventura and G.A. Carvalho, *An updated view and perspectives on high-energy gamma-ray emission from SGR J1935+2154 and its environment*, *JCAP* **2022** (2022) 041 [2204.09734].
- [17] A. de Luca, R.P. Mignani, A. Sartori, W. Hummel, P.A. Caraveo, S. Mereghetti et al., *HST and VLT observations of the neutron star 1E 1207.4-5209*, *A&A* **525** (2011) A106 [1007.3623].
- [18] T.A. Porter, G. Jóhannesson and I.V. Moskalenko, *The GALPROP Cosmic-ray Propagation and Nonthermal Emissions Framework: Release v57*, *ApJS* **262** (2022) 30 [2112.12745].
- [19] L.K. Eppens, J.A. Combi, E.M. Reynoso, F. García, E. Mestre, L. Abaroa et al., *A high-energy study of the supernova remnant G296.5+10.0*, *MNRAS* **528** (2024) 2095.
- [20] M. Araya, *Detection of gamma-ray emission in the region of the supernova remnants G296.5+10.0 and G166.0+4.3*, *MNRAS* **434** (2013) 2202 [1306.5619].
- [21] H. Zeng, Y. Xin, S. Zhang and S. Liu, *TeV Cosmic-Ray Nucleus Acceleration in Shell-type Supernova Remnants with Hard γ -Ray Spectra*, *ApJ* **910** (2021) 78 [2102.03465].
- [22] J.P. Halpern and E.V. Gotthelf, *The First Glitch in a Central Compact Object Pulsar: 1E 1207.4-5209*, in *AAS/High Energy Astrophysics Division*, vol. 17 of *AAS/High Energy Astrophysics Division*, p. 112.50, Mar., 2019.
- [23] V.E. Zavlin, G.G. Pavlov and D. Sanwal, *Variations in the Spin Period of the Radio-quiet Pulsar 1E 1207.4-5209*, *ApJ* **606** (2004) 444 [astro-ph/0312096].
- [24] B. Gong, *Radio-quiet neutron star 1E 1207.4-5209 : a possible strong gravitational-wave source.*, *PRL* **95** (2005) 1101 [astro-ph/0506431].
- [25] E.B. Giacani, G.M. Dubner, A.J. Green, W.M. Goss and B.M. Gaensler, *The Interstellar Matter in the Direction of the Supernova Remnant G296.5+10.0 and the Central X-Ray Source 1E 1207.4-5209*, *Astronomical Journal* **119** (2000) 281.
- [26] S. Mereghetti, A. De Luca, P.A. Caraveo, W. Becker, R. Mignani and G.F. Bignami, *Pulse Phase Variations of the X-Ray Spectral Features in the Radio-quiet Neutron Star 1E 1207-5209*, *ApJ* **581** (2002) 1280 [astro-ph/0207296].
- [27] A. De Luca, S. Mereghetti, P.A. Caraveo, M. Moroni, R.P. Mignani and G.F. Bignami, *XMM-Newton and VLT observations of the isolated neutron star 1E 1207.4-5209*, *A&A* **418** (2004) 625 [astro-ph/0312646].
- [28] V.E. Zavlin, G.G. Pavlov, D. Sanwal and J. Trümper, *Discovery of 424 Millisecond Pulsations from the Radio-quiet Neutron Star in the Supernova Remnant PKS 1209-51/52*, *ApJL* **540** (2000) L25 [astro-ph/0005548].
- [29] A. Moranchel-Basurto, P.F. Velázquez, E. Giacani, J.C. Toledo-Roy, E.M. Schneiter, F. De Colle et al., *Origin of the bilateral structure of the supernova remnant G296.5+10*, *MNRAS* **472** (2017) 2117 [1709.00460].
- [30] R.S. Roger, D.K. Milne, M.J. Kesteven, K.J. Wellington and R.F. Haynes, *Symmetry of the Radio Emission from Two High-Latitude Supernova Remnants, G296.5+10.0 and G324.7+14.6 (SN 1006)*, *ApJ* **332** (1988) 940.
- [31] G.M. Dubner, F.R. Colomb and E.B. Giacani, *1410 MHz continuum and HI line observations towards the SNR G 296.5+10.0 and nearby sources. Evidences of two SNRs tunneling through the interstellar medium.*, *Astronomical Journal* **91** (1986) 343.

- [32] C.J. Hailey and K. Mori, *Evidence of a Mid-Atomic Number Atmosphere in the Neutron Star 1E 1207.4-5209*, *ApJL* **578** (2002) L133 [[astro-ph/0207590](#)].
- [33] A. Ankay, A.M. Ankay and E.N. Ercan, *Possible Evolution of DIM Radio-Quiet Neutron Star 1e 1207.4-5209 Based on a B-Decay Model*, *International Journal of Modern Physics D* **16** (2007) 619 [[0706.0831](#)].
- [34] G.G. Pavlov and V.G. Bezchastnov, *Once-ionized Helium in Superstrong Magnetic Fields*, *ApJL* **635** (2005) L61 [[astro-ph/0505464](#)].
- [35] A.W. Strong, I.V. Moskalenko and V.S. Ptuskin, *Cosmic-Ray Propagation and Interactions in the Galaxy*, *Annual Review of Nuclear and Particle Science* **57** (2007) 285 [[astro-ph/0701517](#)].
- [36] S. Thoudam, J.P. Rachen, A. van Vliet, A. Achterberg, S. Buitink, H. Falcke et al., *Cosmic-ray energy spectrum and composition up to the ankle: the case for a second Galactic component*, *A&A* **595** (2016) A33 [[1605.03111](#)].
- [37] G. Jóhannesson, T.A. Porter and I.V. Moskalenko, *The Three-dimensional Spatial Distribution of Interstellar Gas in the Milky Way: Implications for Cosmic Rays and High-energy Gamma-ray Emissions*, *ApJ* **856** (2018) 45 [[1802.08646](#)].
- [38] T.A. Porter, G. Jóhannesson and I.V. Moskalenko, *High-energy Gamma Rays from the Milky Way: Three-dimensional Spatial Models for the Cosmic-Ray and Radiation Field Densities in the Interstellar Medium*, *ApJ* **846** (2017) 67 [[1708.00816](#)].
- [39] X.H. Sun, W. Reich, A. Waelkens and T.A. Enßlin, *Radio observational constraints on Galactic 3D-emission models*, *A&A* **477** (2008) 573 [[0711.1572](#)].
- [40] A.W. Strong, I.V. Moskalenko and O. Reimer, *Diffuse Continuum Gamma Rays from the Galaxy*, *ApJ* **537** (2000) 763 [[astro-ph/9811296](#)].
- [41] A.W. Strong and I.V. Moskalenko, *Propagation of Cosmic-Ray Nucleons in the Galaxy*, *ApJ* **509** (1998) 212 [[astro-ph/9807150](#)].
- [42] C. Evoli, D. Gaggero, A. Vittino, G. Di Bernardo, M. Di Mauro, A. Ligorini et al., *Cosmic-ray propagation with DRAGON2: I. numerical solver and astrophysical ingredients*, *JCAP* **2017** (2017) 015 [[1607.07886](#)].
- [43] W. Liu, S.-j. Lin, H.-b. Hu, Y.-q. Guo and A.-f. Li, *Two Numerical Methods for the 3D Anisotropic Propagation of Galactic Cosmic Rays*, *ApJ* **892** (2020) 6 [[1909.02908](#)].
- [44] E. Carlson, T. Linden and S. Profumo, *Improved cosmic-ray injection models and the Galactic Center gamma-ray excess*, *PRD* **94** (2016) 063504 [[1603.06584](#)].
- [45] É. Jaupart, É. Parizot and D. Allard, *Contribution of the Galactic centre to the local cosmic-ray flux*, *A&A* **619** (2018) A12 [[1808.02322](#)].
- [46] R.C. Anjos and F. Catalani, *Galactic Center as an efficient source of cosmic rays*, *PRD* **101** (2020) 123015 [[2006.02584](#)].
- [47] G. Jóhannesson, T.A. Porter and I.V. Moskalenko, *Cosmic-Ray Propagation in Light of the Recent Observation of Geminga*, *ApJ* **879** (2019) 91 [[1903.05509](#)].
- [48] D. Malyshev, I. Cholis and J. Gelfand, *Pulsars versus dark matter interpretation of ATIC/PAMELA*, *PRD* **80** (2009) 063005 [[0903.1310](#)].
- [49] D. Atri and B. Hariharan, *Modeling gamma ray production from proton-proton interactions in high-energy astrophysical environments*, *arXiv e-prints* (2013) arXiv:1309.2360 [[1309.2360](#)].
- [50] R. Sasse and R.C. Anjos, *A Connection Between TeV Gamma-ray Flux and Cosmic Rays in the Seyfert Galaxy NGC 1068*, *Acta Phys. Polon. Supp.* **15** (2022) 15.
- [51] A.G.B. Mocellin and R.C. Anjos, *Ultra-high Energy Cosmic Rays Luminosity from Multi-messenger Analysis*, *Acta Phys. Polon. Supp.* **15** (2022) 16.

- [52] G. Jóhannesson, T.A. Porter and I.V. Moskalenko, *The Three-dimensional Spatial Distribution of Interstellar Gas in the Milky Way: Implications for Cosmic Rays and High-energy Gamma-ray Emissions*, *ApJ* **856** (2018) 45 [1802.08646].
- [53] M. Araya, *Detection of gamma-ray emission in the region of the supernova remnants G296.5+10.0 and G166.0+4.3*, *MNRAS* **434** (2013) 2202 [1306.5619].
- [54] Cherenkov Telescope Array Consortium, B.S. Acharya, I. Agudo, I. Al Samarai, R. Alfaro, J. Alfaro et al., *Science with the Cherenkov Telescope Array* (2019), 10.1142/10986.
- [55] M. Aguilar, L. Ali Cavazonza, G. Ambrosi, L. Arruda, N. Attig, F. Barao et al., *The Alpha Magnetic Spectrometer (AMS) on the international space station: Part II - Results from the first seven years*, *Physics Reports* **894** (2021) 1.
- [56] T. Sanuki, M. Motoki, H. Matsumoto, E.S. Seo, J.Z. Wang, K. Abe et al., *Precise Measurement of Cosmic-Ray Proton and Helium Spectra with the BESS Spectrometer*, *ApJ* **545** (2000) 1135 [astro-ph/0002481].
- [57] C. Consolandi, *Precision Measurement of the Proton Flux in Primary Cosmic Rays from 1 GV to 1.8 TV with the Alpha Magnetic Spectrometer on the International Space Station*, *arXiv e-prints* (2016) arXiv:1612.08562 [1612.08562].
- [58] Q. An, R. Asfandiyarov, P. Azzarello, P. Bernardini, X.J. Bi, M.S. Cai et al., *Measurement of the cosmic ray proton spectrum from 40 GeV to 100 TeV with the DAMPE satellite*, *Science Advances* **5** (2019) eaax3793 [1909.12860].
- [59] Y.S. Yoon, T. Anderson, A. Barrau, N.B. Conklin, S. Coutu, L. Derome et al., *Proton and Helium Spectra from the CREAM-III Flight*, *ApJ* **839** (2017) 5 [1704.02512].
- [60] E. Atkin, V. Bulatov, V. Dorokhov, N. Gorbunov, S. Filippov, V. Grebenyuk et al., *New Universal Cosmic-Ray Knee near a Magnetic Rigidity of 10 TV with the NUCLEON Space Observatory*, *Soviet Journal of Experimental and Theoretical Physics Letters* **108** (2018) 5 [1805.07119].
- [61] A.D. Panov, J.H. Adams, H.S. Ahn, G.L. Bashinzhagyan, J.W. Watts, J.P. Wefel et al., *Energy spectra of abundant nuclei of primary cosmic rays from the data of ATIC-2 experiment: Final results*, *Bulletin of the Russian Academy of Sciences, Physics* **73** (2009) 564 [1101.3246].
- [62] F. Alemanno, Q. An, P. Azzarello, F.C.T. Barbato, P. Bernardini, X.J. Bi et al., *Measurement of the Cosmic Ray Helium Energy Spectrum from 70 GeV to 80 TeV with the DAMPE Space Mission*, *PRL* **126** (2021) 201102 [2105.09073].
- [63] M. Aguilar, D. Aisa, B. Alpat, A. Alvino, G. Ambrosi, K. Andeen et al., *Precision Measurement of the Helium Flux in Primary Cosmic Rays of Rigidities 1.9 GV to 3 TV with the Alpha Magnetic Spectrometer on the International Space Station*, *PRL* **115** (2015) 211101.
- [64] M. Aguilar, L. Ali Cavazonza, B. Alpat, G. Ambrosi, L. Arruda, N. Attig et al., *Precision Measurement of Cosmic-Ray Nitrogen and its Primary and Secondary Components with the Alpha Magnetic Spectrometer on the International Space Station*, *PRL* **121** (2018) 051103.
- [65] M. Aguilar, L.A. Cavazonza, M.S. Allen, B. Alpat, G. Ambrosi, L. Arruda et al., *Properties of Iron Primary Cosmic Rays: Results from the Alpha Magnetic Spectrometer*, *PRL* **126** (2021) 041104.
- [66] O. Adriani, Y. Akaike, K. Asano, Y. Asaoka, M.G. Bagliesi, E. Berti et al., *Direct Measurement of the Cosmic-Ray Carbon and Oxygen Spectra from 10 GeV /n to 2.2 TeV /n with the Calorimetric Electron Telescope on the International Space Station*, *PRL* **125** (2020) 251102 [2012.10319].
- [67] J. Chang, J.H. Adams, H.S. Ahn, G.L. Bashinzhagyan, M. Christl, O. Ganel et al., *An excess of cosmic ray electrons at energies of 300-800 GeV*, *Nature* **456** (2008) 362.

- [68] F. Aharonian, A.G. Akhperjanian, G. Anton, U. Barres de Almeida, A.R. Bazer-Bachi, Y. Becherini et al., *Probing the ATIC peak in the cosmic-ray electron spectrum with H.E.S.S.*, *A&A* **508** (2009) 561 [[0905.0105](#)].
- [69] S. Abdollahi, M. Ackermann, M. Ajello, W.B. Atwood, L. Baldini, G. Barbiellini et al., *Cosmic-ray electron-positron spectrum from 7 GeV to 2 TeV with the Fermi Large Area Telescope*, *PRD* **95** (2017) 082007 [[1704.07195](#)].
- [70] DAMPE Collaboration, G. Ambrosi, Q. An, R. Asfandiyarov, P. Azzarello, P. Bernardini et al., *Direct detection of a break in the teraelectronvolt cosmic-ray spectrum of electrons and positrons*, *Nature* **552** (2017) 63 [[1711.10981](#)].
- [71] O. Adriani, Y. Akaike, K. Asano, Y. Asaoka, M.G. Bagliesi, E. Berti et al., *Extended Measurement of the Cosmic-Ray Electron and Positron Spectrum from 11 GeV to 4.8 TeV with the Calorimetric Electron Telescope on the International Space Station*, *PRL* **120** (2018) 261102 [[1806.09728](#)].
- [72] O. Adriani, G.C. Barbarino, G.A. Bazilevskaya, R. Bellotti, M. Boezio, E.A. Bogomolov et al., *Measurement of Boron and Carbon Fluxes in Cosmic Rays with the PAMELA Experiment*, *ApJ* **791** (2014) 93 [[1407.1657](#)].
- [73] O. Adriani, Y. Akaike, K. Asano, Y. Asaoka, E. Berti, G. Bigongiari et al., *Cosmic-Ray Boron Flux Measured from 8.4 GeV/n to 3.8 TeV/n with the Calorimetric Electron Telescope on the International Space Station*, *PRL* **129** (2022) 251103 [[2212.07873](#)].

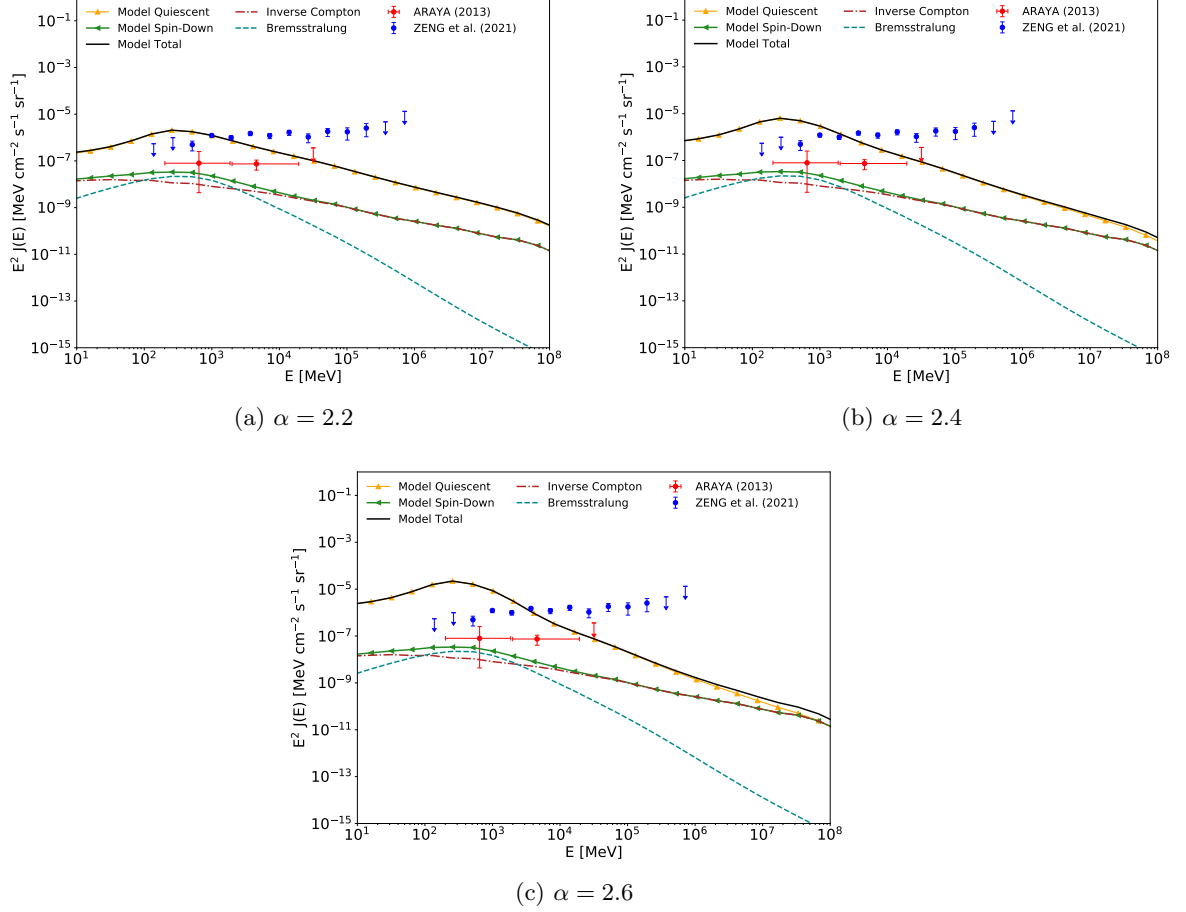


Figure 1: Spectral Energy Distribution of gamma-ray emissions resulting from electrons/positrons in CCO 1E 1207.4-5209 and protons from its associated Supernova Remnant (SNR) G296.5 + 10.0. The model spin-down includes contributions from inverse Compton scattering, and bremsstrahlung. The data points featured in the plots are derived from the model developed by Zeng et al. in 2021 [21] and from gamma-ray measurements conducted by Araya in 2013 [53], focusing on the CCO+SNR association. See text for details. These models utilize a 2D gas distribution as described by Johannesson in 2018 [52].

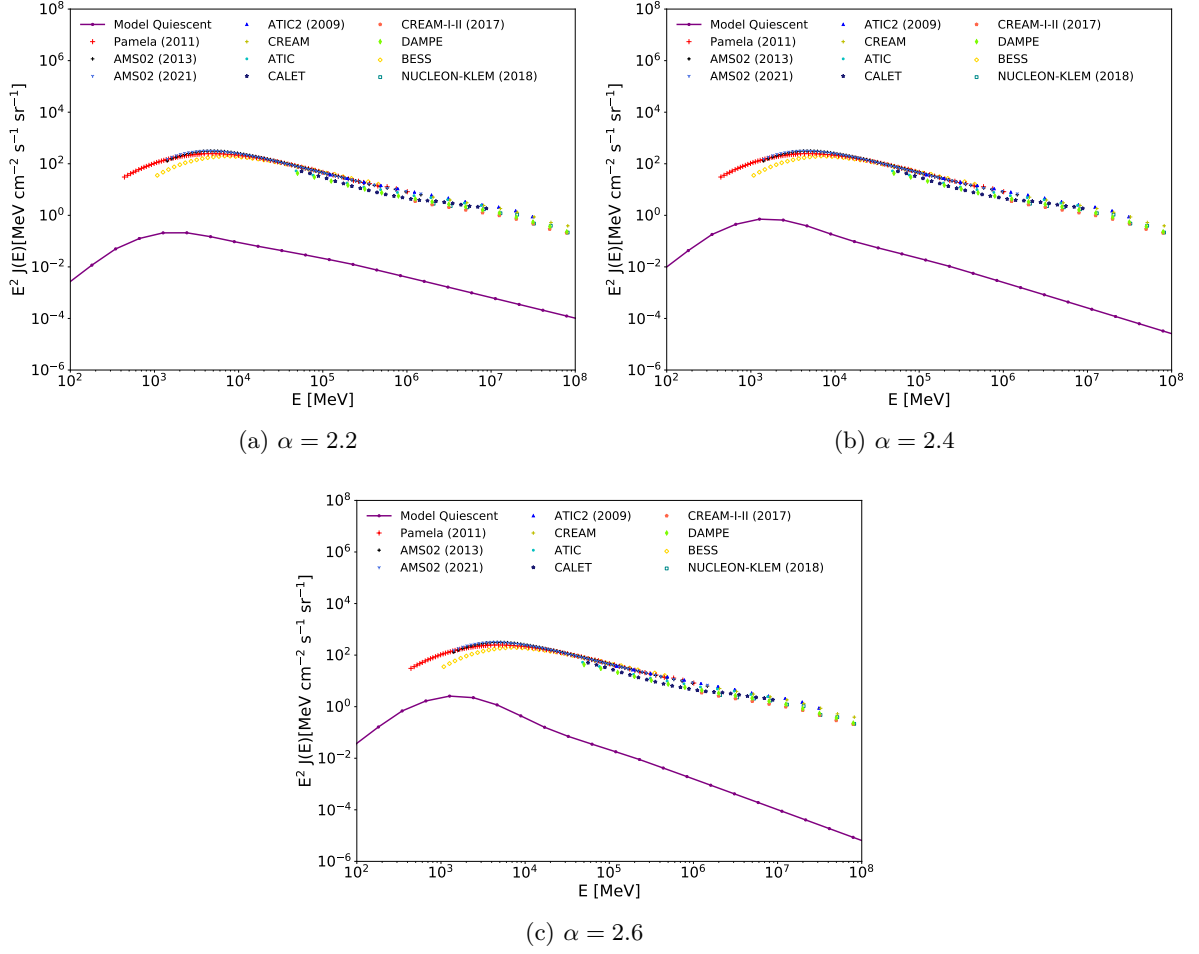


Figure 2: Energy spectra for proton from quiescent model. The spectra are multiplied by E^2 . The models calculations are shown in comparison with the data considering a modulation of 0.30 GV. The data have been extracted from [55–61].

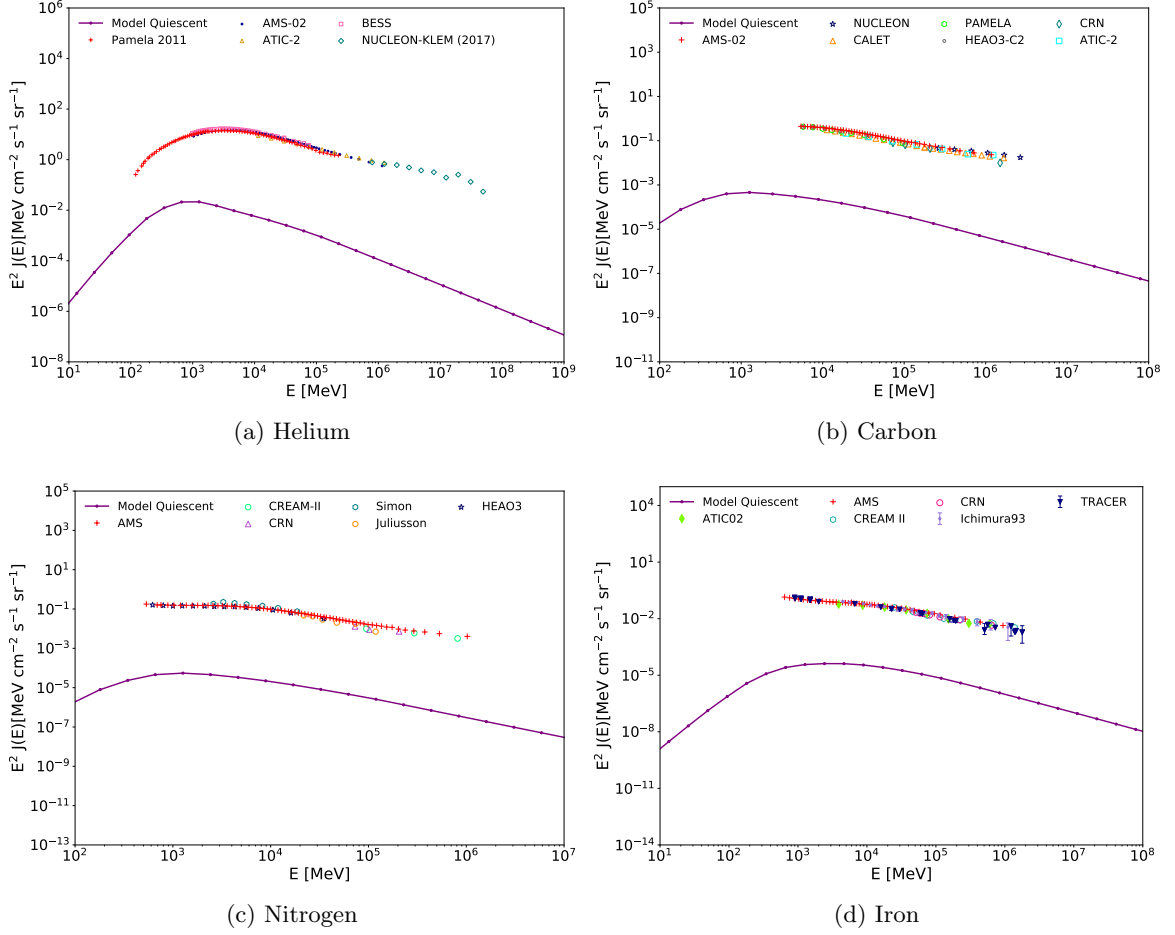


Figure 3: Energy spectra for four elements: helium, carbon, nitrogen and iron from quiescent model. The spectra are multiplied by E^2 . The models calculations are shown in comparison with the data considering spectral index of 2.4 and a modulation of 0.30 GV. The data have been extracted [62–66].

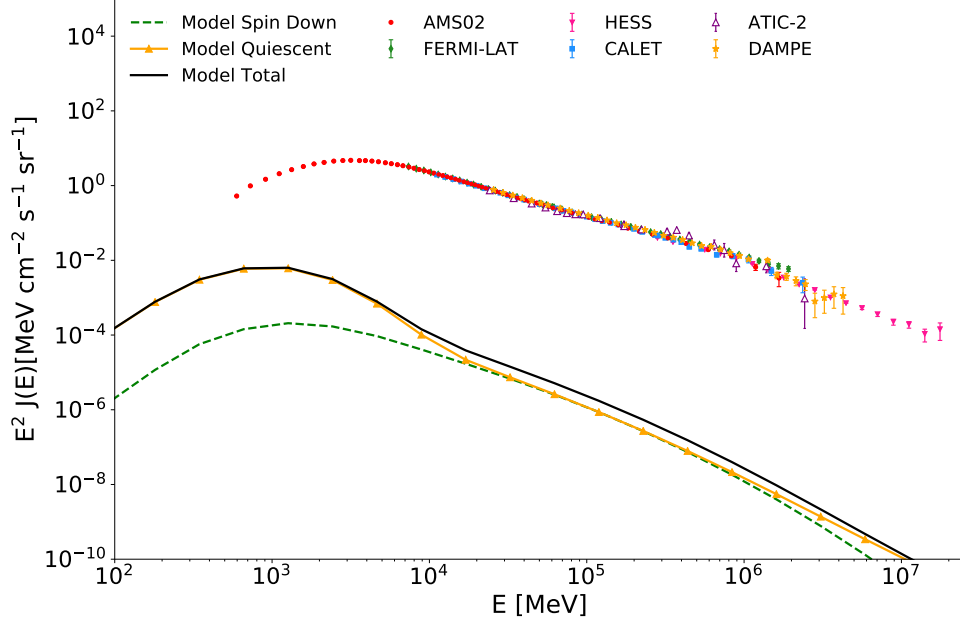


Figure 4: Energy spectra for electron/positron from spin-down and quiescent models. The spectra are multiplied by E^2 . The models are shown in comparison with the data considering spectral index of 2.4 and a modulation of 0.30 GV. The data have been extracted AMS [55], ATIC [67], HESS [68], Fermi-LAT [69], DAMPE [70] and CALET [71].

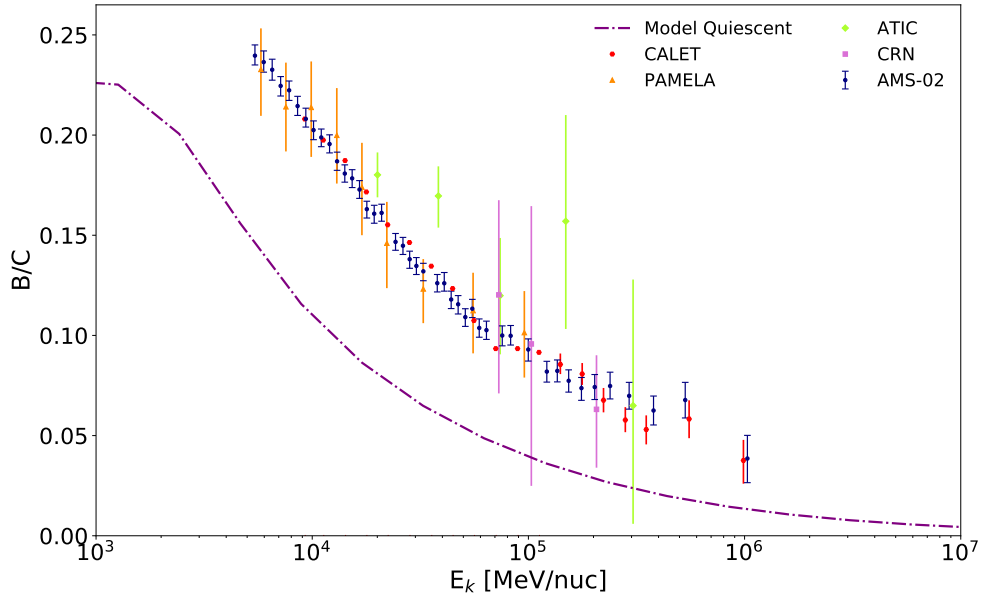


Figure 5: B/C ratio for the quiescent model as a function of kinetic energy per nucleon, displayed in comparison with data from [72, 73].

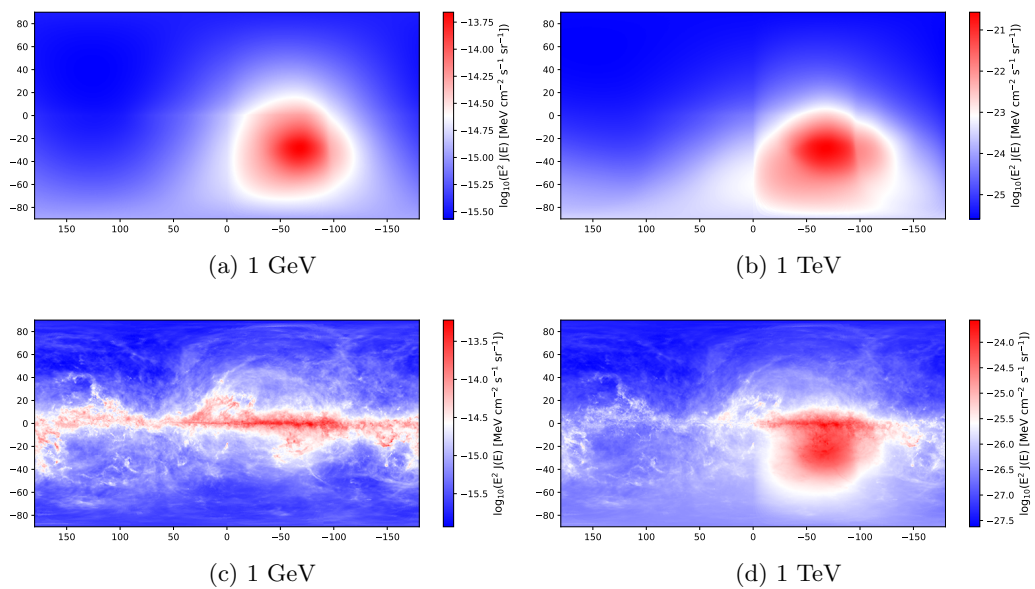


Figure 6: Gamma-ray intensity at 1 GeV and 1 TeV from CCO 1E 1207.4-5209 and its host star SNR G296.5 + 10.0 for the spin-down model. The maps show the production of gamma rays by inverse Compton scattering - (a,b) and bremsstrahlung - (c,d). The maps are in Galactic coordinates with $(l, b) = (0, 0)$ at the center of the map.